

Leveraging Transformers to Improve Breast Cancer Classification and Risk Assessment with Multi-modal and Longitudinal Data

Yiqiu Shen^{1,2,3*}

Jungkyu Park^{3*}

Frank Yeung³

Eliana Goldberg²

Laura Heacock^{2,3}

Farah Shamout^{4,5,6}

Krzysztof J. Geras^{2,3,1}

YS1001@NYU.EDU

JP.PARK@NYU.EDU

FRANK.YEUNG@NYULANGONE.ORG

ELIANA.GOLDBERG@NYULANGONE.ORG

Laura.Heacock@nyulangone.org

FS999@NYU.EDU

K.J.GERAS@NYU.EDU

¹Center for Data Science, New York University, New York, NY, USA

²Department of Radiology, NYU Langone Health, New York, NY, USA

³NYU Grossman School of Medicine, New York, USA

⁴Division of Engineering, New York University Abu Dhabi, Abu Dhabi, UAE

⁵Computer Science and Engineering, New York University, New York, USA

⁶Department of Biomedical Engineering, New York University, New York, USA

Abstract

Breast cancer screening, primarily conducted through mammography, is often supplemented with ultrasound for women with dense breast tissue. However, existing deep learning models analyze each modality independently, missing opportunities to integrate information across imaging modalities and time. In this study, we present Multi-modal Transformer (MMT), a neural network that utilizes mammography and ultrasound synergistically, to identify patients who currently have cancer and estimate the risk of future cancer for patients who are currently cancer-free. MMT aggregates multi-modal data through self-attention and tracks temporal tissue changes by comparing current exams to prior imaging. Trained on 1.3 million exams, MMT achieves an AUROC of 0.943 in detecting existing cancers, surpassing strong uni-modal baselines. For 5-year risk prediction, MMT attains an AUROC of 0.826, outperforming prior mammography-based risk models. Our research highlights the value of multi-modal and longitudinal imaging in cancer diagnosis and risk stratification.

Keywords: breast cancer, deep learning, mammography, ultrasound, multi-modal data

* These authors contributed equally

1. Introduction

Breast cancer is the leading cause of cancer death in women globally. Breast cancer screening aims to detect cancer in its early stage of development so that treatment can lead to better patient outcomes. Despite the wide adoption of full-field digital mammography (FFDM) and digital breast tomosynthesis (DBT), only approximately 75% of breast cancers are diagnosed through mammography (Lee et al., 2021; Monticciolo et al., 2017). This limitation stems from dense breast tissue obscuring smaller tumors and reducing mammography’s sensitivity to as low as 61-65% in women with extremely dense breasts (Mandelson et al., 2000; Wanders et al., 2017; Destounis et al., 2017). These women require supplemental screening to compensate for the limitations of mammography. Ultrasound is commonly used given its accessibility, lower costs, and lack of radiation. While ultrasound does increase cancer detection rates by 3-4 per 1000 women (Berg et al., 2012), this improvement comes at the cost of lower specificity, increased recall rates of 7.5-10.6% (Berg and Vourtsis, 2019; Brem et al., 2015; Butler and Hooley, 2020) and lower positive predictive values (PPV) of 9-11% (Berg and Vourtsis, 2019), leading to unnecessary diagnostic imaging and biopsies. Artificial intelligence presents opportunities to improve precision by synergistically using mammography and ultrasound.

Deep learning models have been applied to support breast cancer screening, primarily through detecting existing cancers (Shen et al., 2021b; Wu et al., 2019; McKinney et al., 2020; Shen et al., 2019a; Lotter et al., 2021; Rodriguez-Ruiz et al., 2019; Lotter et al., 2021) or predicting future risk (Yala et al., 2019, 2021; Arasu et al., 2023; Lehman et al., 2022). Within this area, several seminal studies have made great contributions. McKinney et al. (2020) demonstrated that convolutional neural networks (CNNs) match the screening performance of radiologists and retain generalizability across countries. Yala et al. (2019, 2021) proposed Mirai, an AI system that utilizes mammography and clinical risk factors to forecast the future risk of breast cancer. Shen et al. (2021a) showed that AI can reduce the false-positive rates by 37.3% in breast ultrasound interpretation, without compromising sensitivity.

Despite these advances, there are two major limitations. First, existing work tends to concentrate on a single imaging modality, ignoring cross-modal patterns only noticeable through integrating multiple imaging modalities. In contrast, radiologists often use complementary imaging modalities to ascertain a diagnosis and increase accuracy (Bankman, 2008). Furthermore, existing work overlooks the utility of prior imaging despite that comparison to prior mammograms has been shown to significantly reduce the recall rate and increase cancer detection rate and PPV1 (Hayward et al., 2016).

In this study, we introduce an AI system capable of referencing prior imaging and synthesizing information from both mammography and ultrasound. This system has two functionalities: detecting extant cancers and predicting future cancer risk.

2. Methods

Problem Formulation We formulate breast cancer diagnosis as a sequence classification task. Let S_i denote an imaging exam with images $I_i^1, I_i^2, \dots, I_i^{l_i}$, where l_i denotes the number of images in S_i . Let m_i denote S_i 's imaging modality and t_i denote the time when S_i is performed. S_i has prior exams $S_i^1, S_i^2, \dots, S_i^{r_i}$, all of which belong to the same patient but were performed at the same or earlier times $t_i^1, t_i^2, \dots, t_i^{r_i} \leq t_i$, where r_i is the number of prior exams. Our goal is to build an AI system that takes the sequence $Q_i = \{S_i, S_i^1, S_i^2, \dots, S_i^{r_i}\}$ as an input and makes a series of probabilistic predictions $\hat{y}_i^j \in [0, 1]$ quantifying the probability of malignancy within 120

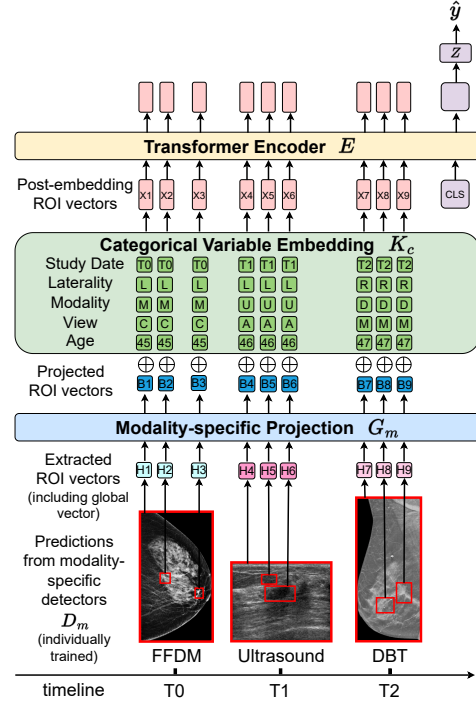


Figure 1: Architecture of MMT.

days ($j = 0$) and each of 1 to 5 years ($j = 1, 2, \dots, 5$) from t_i .

There are two key challenges. First, each patient has a unique exam history (hence a unique set of imaging modalities) with variable numbers of images. The model must handle this variability. Second, malignant lesions have diverse visual patterns across modalities. The model must capture this spectrum and integrate findings across imaging modalities.

Multi-modal Transformer We propose the Multi-modal Transformer (MMT) to address the aforementioned challenges. As illustrated in Figure 1, MMT produces cancer predictions in three steps. First, MMT applies modality-specific detectors to all images to extract feature vectors from regions that are suspicious of cancer. Second, it combines these features with embeddings of non-image variables. Finally, the post-embedding features are fed into a transformer encoder to detect temporal changes in tissue patterns, integrate multi-modal tissue information, and produce malignancy predictions. The following paragraphs elaborate on each step in detail.

Generating regions of interest and feature vectors. A typical input sequence Q_i contains images of multi-

ple modalities. Since tumor morphology varies across modalities, we train a detector D_m for each modality $m \in \{\text{FFDM, DBT, Ultrasound}\}$. Each D_m takes an image I as input and outputs k_m regions of interest (ROIs) with feature representations $H \in \mathbb{R}^{k_m, d_m}$ and scores $P_c \in \mathbb{R}^{k_m}$, reflecting its belief that each ROI contains a malignant lesion. Only the top k_m highest scoring ROIs are extracted, where k_m is a hyper-parameter that is tuned on the validation set. Some detectors also produce global feature vectors. As feature vectors are extracted by different D_m , they vary in size and scale. To address this, we apply a modality-specific transform G_m (a multilayer perceptron) to project all features into the same space: $B = G_m(H)$, where $B \in \mathbb{R}^{k_m, d}$ denotes the post-projection feature vectors.

Categorical embeddings. We incorporate categorical variables including study date, laterality, imaging modality, imaging view angles, and patient age discretized into ranges. These variables help our model understand the temporal and spatial patterns in the ROI patches. We utilize the embedding technique to map each variable c to an embedding vector $K_c \in \mathbb{R}^{100}$, which are then concatenated with the post-projection ROI feature vectors. Next, we use a multilayer perceptron $f_{\text{emb}} : \mathbb{R}^{d+500} \mapsto \mathbb{R}^d$ to reduce dimensionality:

$$X = f_{\text{emb}}([B, K_{\text{date}}, K_{\text{lat}}, K_{\text{mod}}, K_{\text{view}}, K_{\text{age}}]^T), \quad (1)$$

where $X \in \mathbb{R}^{k_m, d}$ denote post-embedding vectors.

Transformer. We use a transformer encoder to enable interaction among post-embedding ROI vectors from all images (Vaswani et al., 2017). The transformer encoder uses multi-head attention to selectively combine information from the input sequence. As a common practice (Devlin et al., 2018), we inject a special CLS token into the input sequence. The CLS token condenses variable-length input sequences into a fixed-size aggregated representation and allows the transformer to iteratively update it using signals from all post-embedding ROI vectors:

$$\text{CLS}' = \text{transformer}([X, \text{CLS}]). \quad (2)$$

Next, we apply a multi-layer perceptron $Z : \mathbb{R}^d \mapsto \mathbb{R}^6$ with a rectified linear unit (ReLU) on the post-transformer CLS vector (CLS') to generate six non-negative risk scores for non-overlapping intervals: baseline risk within 120 days (L^0), additional 120d-1yr risk (L^1), 1-2yr risk (L^2), 2-3yr risk (L^3), 3-4yr risk (L^4), and 4-5yr risk (L^5). This is expressed in

the equation below:

$$[L^0, L^1, L^2, L^3, L^4, L^5]^T = \text{ReLU}(Z(\text{CLS}')). \quad (3)$$

Finally, we use an additive hazard layer (Aalen and Scheike, 2005) with sigmoid non-linearity to generate the cumulative probability of malignancy:

$$\hat{y}^j = \sigma(L^0 + \sum_{k=1}^j L_k). \quad (4)$$

Training MMT is trained in two phases. First, for each modality, we independently train cancer detectors using only images from that modality. FFDM and DBT detectors are parameterized as YOLOX (Ge et al., 2021), MogaNet (Li et al., 2022), and GMIC (Shen et al., 2021a, 2019b). YOLOX is an anchor-free version of YOLO (Redmon et al., 2016), a popular object detection model family. MogaNet is a CNN that can efficiently model interactions among visual features. GMIC is a resource-efficient CNN that is designed for high-resolution medical images. For DBT, we train on 2D slices to limit computation. YOLOX and MogaNet detectors are trained on both image and bounding box labels. To train with image labels, we attention-pool the features of the highest-scoring boxes and classify them using a logistic regression layer. We use the UltraNet proposed in Shen et al. (2021a) as our ultrasound detector. To balance computation cost, we extracted 10 ROIs from each image across modalities.

In the second phase, we freeze detectors and train the transformer encoder, MLPs, and embeddings on multi-modal sequences using binary cross-entropy loss and Adam optimizer (Kingma and Ba, 2014) with a learning rate set to 10^{-5} .

Ensembling To improve results, we use model ensembling (Dietterich, 2000). We train 100 MMT models, randomly combining one model from each detector family with a transformer encoder that is randomly parameterized as either a DeiT (Touvron et al., 2021), a ViT (Dosovitskiy et al., 2020), or a BERT (Devlin et al., 2018). The top 5 MMT models by validation performance are ensemble averaged to produce the final prediction.

3. Results

Dataset We trained and evaluated our model on the NYU Breast Cancer Diagnosis Multi-modal Dataset containing 1,353,521

FFDM/DBT/ultrasound exams from 297,751 patients who visited NYU Langone Health between 2010 and 2020. Exams are split into training (87.1%), validation (3.9%), and test (8.9%) sets, with each patient’s exams assigned to only one set. Labels indicating presence or absence of cancer are derived from corresponding pathology reports. Validation and test sets are filtered so cancer-positive exams have pathology confirmation and cancer-negative exams have a negative follow-up. See Table A2 for dataset details.

Evaluation We evaluate our model’s ability to detect existing cancers and predict risk in the general screening population. Each test case is a screening visit with required FFDM and optional DBT/ultrasound. Our model utilizes all available modalities and prior studies. For detection of existing cancer, a visit is cancer-positive if a pathology study within 120 days of imaging confirms cancer. The 121,037 exams in the test set came from 54,789 screening visits, out of which 483 led to cancer diagnosis. Among these visits, 26,028 (47.5%) had same-day DBT, 15,542 (28.4%) had same-day ultrasound, and 34,888 (63.7%) had prior imaging studies available. On average, each visit had 1.9 associated prior imaging exams. For 5-year risk stratification, we exclude screening-detected cancers and negative cases with < 5-year follow-up, focusing solely on long-term prediction. This leaves 6,173 visits with 598 positive cases in the test set. We use area under the ROC curve (AUROC) and area under the precision-recall curve (AUPRC) as evaluation metrics.

Performance For cancer diagnosis, we compared MMT to four baselines – GMIC, YOLOX, and MogaNet using FFDM only, and a multi-modal ensemble averaging predictions from the mammogram baselines and UltraNet, when ultrasound is available. For each uni-modal baseline, we trained 20 models and ensembled the top 5 for evaluation. We report the performance in Table 1. MMT achieved higher AUROC and AUPRC than mammogram-only baselines, indicating that incorporating ultrasound improves diagnostic accuracy. MMT also outperformed the multi-modal ensemble, indicating the transformer integrates multi-modal information better than simple averaging.

For risk stratification, we compared MMT to two baselines: radiologists’ BI-RADS diagnosis and Mirai (Yala et al., 2021), an AI system predicting future breast cancer risk using both categorical risk

Table 1: Cancer diagnosis performance.

Model	AUROC	AUPRC
GMIC (Shen et al., 2021b)	0.866	0.167
YOLOX (Ge et al., 2021)	0.876	0.172
MogaNet (Li et al., 2022)	0.874	0.181
Multi-modal Ensemble	0.925	0.251
MMT	0.943	0.518

factors and mammograms, on the same test set. We report the performance in Table 2. For 5-year cancer prediction, MMT achieved an AUROC of 0.826 and AUPRC of 0.524, outperforming both methods. By leveraging multi-modal imaging and longitudinal patient history, MMT demonstrates a strong ability to predict future breast cancer risk.

Table 2: Risk stratification performance.

Model	AUROC	AUPRC
BI-RADS	0.585	0.118
Mirai (Yala et al., 2019)	0.732	0.252
MMT	0.826	0.524

Ablation Study We performed an ablation study to understand the impact of supplemental modalities and prior imaging. We evaluated MMT using only mammograms with prior imaging (mammo only), using both mammograms and ultrasound but with no prior imaging (no prior), and incorporating only 1, 2, or 3 years of prior imaging. As shown in Table 3, compared to mammograms alone, MMT shows meaningful performance gains when ultrasound is also used for both tasks, confirming the importance of supplemental modality. In contrast, prior imaging mainly contributes to long-term risk stratification. Moreover, prior imaging beyond two years provides only marginal improvement. This observation is consistent with the clinical practice of using up to two years as references. Overall, the ablation highlights the value of multi-modal and longitudinal information, with ultrasound and recent prior imaging improving cancer diagnosis and risk prediction.

4. Discussion and conclusion

In medical imaging, each modality has its own strengths and limitations. Radiologists often combine multiple modalities to inform decision-making. In this spirit, we propose MMT to jointly utilize mam-

Table 3: Ablation study on the impact of supplemental modality and prior imaging.

Model	Cancer Diagnosis		Risk Stratification	
	AUROC	AUPRC	AUROC	AUPRC
mammo only	0.925	0.373	0.814	0.516
no prior	0.944	0.484	0.817	0.513
1 year prior	0.944	0.487	0.816	0.514
2 year prior	0.945	0.507	0.822	0.521
3 year prior	0.944	0.512	0.825	0.523
MMT	0.943	0.518	0.826	0.524

mography and ultrasound for breast cancer screening. MMT achieves strong performance in identifying existing cancers and predicting long-term risk.

Standard-of-care risk models use personal history, genetics, family history, and breast density to estimate risk, but exhibit suboptimal accuracy (Arasu et al., 2023). This stems from their reliance on coarse variables that inadequately capture underlying breast tissue heterogeneity associated with cancer risk. Our study demonstrates that integrating multi-modal longitudinal patient data with neural networks can significantly improve risk modeling by extracting richer tissue features predictive of cancer development.

This study also has limitations. First, we did not evaluate our model on external datasets, which is necessary to demonstrate its generalizability across diverse patient populations and acquisition protocols. Additionally, our model uses primarily imaging data. Incorporating risk factors like demographics and family history could further enhance risk modeling. Addressing these limitations through multi-institutional studies, and integrating non-imaging data will be important future directions to translate these promising results into clinical practice.

5. Acknowledgements

This research was supported by the National Institutes of Health (NIH), through grants TL1TR001447 (the National Center for Advancing Translational Sciences) and P41EB017183, the Gordon and Betty Moore Foundation (9683), and the National Science Foundation (1922658). The content is solely the responsibility of the authors and does not necessarily represent the official views of any of the bodies funding this work.

References

- Odd O Aalen and Thomas H Scheike. Aalen’s additive regression model. *Encyclopedia of biostatistics*, 1, 2005.
- Vignesh A Arasu, Laurel A Habel, Ninah S Achacoso, Diana SM Buist, Jason B Cord, Laura J Esserman, Nola M Hylton, M Maria Glymour, John Kornak, Lawrence H Kushi, et al. Comparison of mammography ai algorithms with a clinical risk model for 5-year breast cancer risk prediction: An observational study. *Radiology*, 307(5):e222733, 2023.
- Isaac Bankman. *Handbook of medical image processing and analysis*. Elsevier, 2008.
- Wendie A Berg and Athina Vourtsis. Screening breast ultrasound using handheld or automated technique in women with dense breasts. *Journal of breast imaging*, 1(4):283–296, 2019.
- Wendie A Berg, Zheng Zhang, Daniel Lehrer, Roberta A Jong, Etta D Pisano, Richard G Barr, Marcela Böhm-Vélez, Mary C Mahoney, W Phil Evans, Linda H Larsen, et al. Detection of breast cancer with addition of annual screening ultrasound or a single screening mri to mammography in women with elevated breast cancer risk. *Journal of the American medical association*, 307(13):1394–1404, 2012.
- Rachel F Brem, Megan J Lenihan, Jennifer Lieberman, and Jessica Torrente. Screening breast ultrasound: past, present, and future. *American Journal of Roentgenology*, 204(2):234–240, 2015.
- Reni S Butler and Regina J Hooley. Screening breast ultrasound: update after 10 years of breast density notification laws. *American Journal of Roentgenology*, 214(6):1424–1435, 2020.
- Stamatia Destounis, Lisa Johnston, Ralph Highnam, Andrea Arieno, Renee Morgan, and Ariane Chan. Using volumetric breast density to quantify the potential masking risk of mammographic density. *American journal of roentgenology*, 208(1):222–227, 2017.
- Jacob Devlin, Ming-Wei Chang, Kenton Lee, and Kristina Toutanova. Bert: Pre-training of deep bidirectional transformers for language understanding. *arXiv*, 2018.

- Thomas G Dietterich. Ensemble methods in machine learning. In *International workshop on multiple classifier systems*, pages 1–15. Springer, 2000.
- Alexey Dosovitskiy, Lucas Beyer, Alexander Kolesnikov, Dirk Weissenborn, Xiaohua Zhai, Thomas Unterthiner, Mostafa Dehghani, Matthias Minderer, Georg Heigold, Sylvain Gelly, et al. An image is worth 16x16 words: Transformers for image recognition at scale. *arXiv*, 2020.
- Zheng Ge, Songtao Liu, Feng Wang, Zeming Li, and Jian Sun. YoloX: Exceeding yolo series in 2021. *arXiv*, 2021.
- Jessica H Hayward, Kimberly M Ray, Dorota J Wisner, John Kornak, Weiwen Lin, Edward A Sickles, and Bonnie N Joe. Improving screening mammography outcomes through comparison with multiple prior mammograms. *American journal of roentgenology*, 207(4):918, 2016.
- Diederik P Kingma and Jimmy Ba. Adam: A method for stochastic optimization. *arXiv*, 2014.
- Cindy S Lee, Linda Moy, Danny Hughes, Dan Golden, Mythreyi Bhargavan-Chatfield, Jennifer Hemingway, Agnieszka Geras, Richard Duszak, and Andrew B Rosenkrantz. Radiologist characteristics associated with interpretive performance of screening mammography: a national mammography database (nmd) study. *Radiology*, 300(3):518–528, 2021.
- Constance D Lehman, Sarah Mercaldo, Leslie R Lamb, Tari A King, Leif W Ellisen, Michelle Specht, and Rulla M Tamimi. Deep learning vs traditional breast cancer risk models to support risk-based mammography screening. *Journal of the National Cancer Institute*, 114(10):1355–1363, 2022.
- Siyuan Li, Zedong Wang, Zicheng Liu, Cheng Tan, Haitao Lin, Di Wu, Zhiyuan Chen, Jiangbin Zheng, and Stan Z Li. Efficient multi-order gated aggregation network. *arXiv*, 2022.
- William Lotter, Abdul Rahman Diab, Bryan Haslam, Jiye G Kim, Giorgia Grisot, Eric Wu, Kevin Wu, Jorge Onieva Onieva, Yun Boyer, Jerrold L Boxerman, et al. Robust breast cancer detection in mammography and digital breast tomosynthesis using an annotation-efficient deep learning approach. *Nature medicine*, 27(2):244–249, 2021.
- Margaret T Mandelson, Nina Oestreicher, Peggy L Porter, Donna White, Charles A Finder, Stephen H Taplin, and Emily White. Breast density as a predictor of mammographic detection: comparison of interval-and screen-detected cancers. *Journal of the National Cancer Institute*, 92(13):1081–1087, 2000.
- Scott Mayer McKinney, Marcin Sieniek, Varun Godbole, Jonathan Godwin, Natasha Antropova, Hutan Ashrafian, Trevor Back, Mary Chesus, Greg S Corrado, Ara Darzi, et al. International evaluation of an ai system for breast cancer screening. *Nature*, 577(7788):89–94, 2020.
- Debra L Monticciolo, Mary S Newell, R Edward Hendrick, Mark A Helvie, Linda Moy, Barbara Monsees, Daniel B Kopans, Peter R Eby, and Edward A Sickles. Breast cancer screening for average-risk women: recommendations from the acr commission on breast imaging. *Journal of the American college of radiology*, 14(9):1137–1143, 2017.
- Joseph Redmon, Santosh Divvala, Ross Girshick, and Ali Farhadi. You only look once: Unified, real-time object detection. In *Proceedings of the IEEE conference on computer vision and pattern recognition*, pages 779–788, 2016.
- Alejandro Rodriguez-Ruiz, Kristina Lång, Albert Gubern-Merida, Mireille Broeders, Gisella Genaro, Paola Clauser, Thomas H Helbich, Margarita Chevalier, Tao Tan, Thomas Mertelmeier, et al. Stand-alone artificial intelligence for breast cancer detection in mammography: comparison with 101 radiologists. *Journal of the National Cancer Institute*, 111(9):916–922, 2019.
- Li Shen, Laurie R Margolies, Joseph H Rothstein, Eugene Fluder, Russell McBride, and Weiva Sieh. Deep learning to improve breast cancer detection on screening mammography. *Scientific reports*, 9(1):12495, 2019a.
- Yiqiu Shen, Nan Wu, Jason Phang, Jungkyu Park, Gene Kim, Linda Moy, Kyunghyun Cho, and Krzysztof J Geras. Globally-aware multiple instance classifier for breast cancer screening. In *Machine learning in medical imaging*, pages 18–26. Springer, 2019b.
- Yiqiu Shen, Farah E Shamout, Jamie R Oliver, Jan Witowski, Kawshik Kannan, Jungkyu Park, Nan

- Wu, Connor Huddleston, Stacey Wolfson, Alexandra Millet, et al. Artificial intelligence system reduces false-positive findings in the interpretation of breast ultrasound exams. *Nature communications*, 12(1):5645, 2021a.
- Yiqiu Shen, Nan Wu, Jason Phang, Jungkyu Park, Kangning Liu, Sudarshini Tyagi, Laura Heacock, S Gene Kim, Linda Moy, Kyunghyun Cho, et al. An interpretable classifier for high-resolution breast cancer screening images utilizing weakly supervised localization. *Medical image analysis*, 68: 101908, 2021b.
- Hugo Touvron, Matthieu Cord, Matthijs Douze, Francisco Massa, Alexandre Sablayrolles, and Hervé Jégou. Training data-efficient image transformers & distillation through attention. In *International conference on machine learning*, pages 10347–10357. PMLR, 2021.
- Ashish Vaswani, Noam Shazeer, Niki Parmar, Jakob Uszkoreit, Llion Jones, Aidan N Gomez, Lukasz Kaiser, and Illia Polosukhin. Attention is all you need. *Advances in neural information processing systems*, 30, 2017.
- Johanna OP Wanders, Katharina Holland, Wouter B Veldhuis, Ritse M Mann, Ruud M Pijnappel, Petra HM Peeters, Carla H van Gils, and Nico Karssemeijer. Volumetric breast density affects performance of digital screening mammography. *Breast cancer research and treatment*, 162:95–103, 2017.
- Nan Wu, Jason Phang, Jungkyu Park, Yiqiu Shen, Zhe Huang, Masha Zorin, Stanislaw Jastrzebski, Thibault Fevry, Joe Katsnelson, Eric Kim, et al. Deep neural networks improve radiologists’ performance in breast cancer screening. *IEEE transactions on medical imaging*, 39(4):1184–1194, 2019.
- Adam Yala, Constance Lehman, Tal Schuster, Tally Portnoi, and Regina Barzilay. A deep learning mammography-based model for improved breast cancer risk prediction. *Radiology*, 292(1):60–66, 2019.
- Adam Yala, Peter G Mikhael, Fredrik Strand, Gigin Lin, Kevin Smith, Yung-Liang Wan, Leslie Lamb, Kevin Hughes, Constance Lehman, and Regina Barzilay. Toward robust mammography-based models for breast cancer risk. *Science translational medicine*, 13(578):eaba4373, 2021.

Table A1: Performance of MMT on patient subgroups stratified by age and breast density.

	AUROC (cancer diagnosis)	AUROC (risk stratification)
Age		
<50 years old	0.927	0.820
50-60 years old	0.957	0.790
60-70 years old	0.941	0.810
70-80 years old	0.920	0.830
>80 years old	0.928	0.965
Breast Density		
A	0.967	0.776
B	0.949	0.813
C	0.936	0.824
D	0.921	0.838

Table A2: Characteristics of the NYU Breast Cancer Diagnosis Multi-modal Dataset.

	Training	Validation	Test
Patients	263,573	10,839	23,339
Age, mean years (SD)	56.98 (13.09)	59.58 (11.55)	59.77 (11.47)
<40 yr old	17,186 (6.52%)	173 (1.60%)	351 (1.50%)
40-49 yr old	63,158 (23.96%)	2,308 (21.29%)	4,806 (20.59%)
50-59 yr old	64,882 (24.62%)	3,088 (28.49%)	6,679 (28.62%)
60-69 yr old	54,980 (20.86%)	2,960 (27.31%)	6,582 (28.20%)
≥ 70 yr old	43,022 (16.32%)	2,092 (19.30%)	4,582 (19.63%)
Unkown	20,345 (7.72%)	218 (2.01%)	339 (1.45%)
Breast density			
A	18,616 (7.06%)	773 (7.13%)	1,756 (7.52%)
B	93,990 (35.66%)	4,225 (38.98%)	9,415 (40.34%)
C	113,631 (43.11%)	5,005 (46.18%)	10,542 (45.17%)
D	16,991 (6.45%)	618 (5.70%)	1,287 (5.51%)
Unkown	20,345 (7.72%)	218 (2.01%)	339 (1.45%)
Exams			
cancer 120 days	15,586 (1.32%)	877 (1.65%)	1,902 (1.57%)
cancer 120 days - 1 year	1,566 (0.13%)	19 (0.04%)	13 (0.01%)
cancer 1-2 years	4,816 (0.41%)	54 (0.10%)	133 (0.11%)
cancer 2-3 years	3,417 (0.29%)	249 (0.47%)	613 (0.51%)
cancer 3-4 years	2,089 (0.18%)	182 (0.34%)	364 (0.30%)
cancer 4-5 years	1,281 (0.11%)	101 (0.19%)	248 (0.20%)
cancer >5 years	1,391 (0.12%)	92 (0.17%)	268 (0.22%)
Imaging modality			
FFDM	546,862 (46.38%)	26,687 (50.06%)	62,249 (51.43%)
DBT	300,277 (25.47%)	12,139 (22.77%)	28,339 (23.41%)
Ultrasound	332,032 (28.16%)	14,487 (27.17%)	30,449 (25.16%)
Exam-level BI-RADS			
0	439,112 (10.99%)	19,811 (9.66%)	45,060 (9.57%)
1	439,112 (37.24%)	19,811 (37.16%)	45,060 (37.23%)
2	501,915 (42.57%)	24,598 (46.14%)	56,810 (46.94%)
3	70,935 (6.02%)	1,683 (3.16%)	3,453 (2.85%)
4	33,517 (2.84%)	1,999 (3.75%)	4,002 (3.31%)
5	2,535 (0.21%)	73 (0.14%)	129 (0.11%)
6	1,611 (0.14%)	0 (0.00%)	0 (0.00%)